Materials Research Proceedings 31 (2023) 29-37 https://doi.org/10.21741/9781644902592-4

Progressive failure analysis of postbuckled plates via mixed formulation

Riccardo Vescovini[1,a *], Mohammad Reza Najafian Zadeh Najafabadi[1,b]

[1]Politecnico di Milano Department of Aerospace Science and Technology, Via La Masa 34 20156, Milano, Italy

[a]riccardo.vescovini@polimi.it, [b]mohammadreza.najafian@polimi.it

Keywords: Progressive Failure Analysis, Mixed Formulation, Semi-Analytical Methods, Ritz Method, Elastic Couplings

Abstract. This paper presents a strategy for Progressive Failure Analysis (PFA) of laminated plates, including Variable Stiffness ones, based on the Ritz method. The formulation is developed using a mixed variational principle, where the unknowns are the stress function and the out-of-plane deflections. A linear degradation model is implemented to account for damage evolution. To ensure accurate predictions, emphasis is placed on the method's ability to correctly handle the laminate's elastic couplings. The iterative nature of this type of analysis is effectively managed due to the reduced number of degrees of freedom required. Exemplary results are reported, and comparisons with Abaqus results are provided to demonstrate the quality of the predictions.

Introduction

Thin plates are elementary structural components of many engineering structures, including those employed in aerospace constructions. In this field, lightweight designs are of crucial importance and, for this purpose, it is beneficial to exploit the plate load-carrying capabilities in the postbuckling field. Indeed, after the panel buckles, internal stress redistribution allows further loads to be sustained. The failure mechanisms of composite panels can be relatively complex and may involve geometrically and materially nonlinear phenomena such as mode-jumping, intra- and inter-laminar failures − independent on each other or in combination. The behavior can be even more complex due to internal load redistribution mechanisms arising from the interaction with the surrounding parts of the structure, such as in the case of the local buckling of stringers [1].

Simplified approaches, such as the ones based on the effective width concept, are a useful mean for predicting the failure load in the preliminary design phases. These strategies offer the potential to obtain an estimate of the loads, but, for many purposes, tend to be oversimplified. The designers would benefit from the availability of more advanced tools, where insight can be gathered into the underlying mechanisms leading the structure to the failure. These considerations are even more true for the composite structures of the next generation based on the Variable Stiffness (VS) concept [2,3]. The availability of more design variables, as well as the possibility of tailoring the internal load paths, make the adoption of fast yet accurate tools even more appealing.

Continuum Damage Mechanics (CDM) is a well-consolidated framework for modeling damage response at macro-scale level and predicting failure in composites. Matzenmiller et al. [4] proposed a degradation procedure for fiber-reinforced composites exhibiting elastic-brittle behavior. Based on his work, Lapczyk and Hurtado [5] presented a linear damage evolution law with focus on finite element implementation. A few studies in the past have shown that CDM can be successfully coupled also with semi-analytical methods to simulate progressive damage modeling of postbuckled composite plates [6,7]. All previous works in this context are restricted to isotropic plates and classical straight-fiber composite laminates. To the best of the authors' knowledge, a recent work by Campagna et al. [8] is the only attempt to account for VS configurations too. The Ritz model of [8] refers to a displacement-based approach and allows for improved computational

efficiency. In the present effort, a Ritz method is developed along with continuum damage capabilities. As opposed to [8], the formulation proposed here refers to a unitary variational principle based on a mixed formulation [9,10,11], the main advantage being the reduction of the unknown fields from five to two. This framework is extended here, for the first time, to account for a CDM model aiming at achieving improved failure load prediction capabilities. The proposed extension not only involves the implementation of the damage model, but includes a novel strategy to appropriately account for elastic couplings that can affect the accuracy of the predicted failure load and the identification of the critical spots.

Mixed Formulation

Goal of this investigation is the failure analysis of Variable Stiffness plates operating in the postbuckling field. These plates are characterized by nonuniform elastic properties, hence appropriate methods capable of capturing any relevant elastic coupling effect are of concern. The plate is assumed to be thin such that Kirchhoff assumptions can be applied. The dimensions are defined with l_x and l_y, while the thickness is h. The layup is symmetric, so membrane and bending anisotropy effects can be considered. These effects play an important role in the plate failure mechanisms, as discussed later.

The plate model aims to represent the skin of a stiffened panel, such as those employed in aeronautical structures. Any set of flexural boundary conditions can be considered, i.e. clamped, free or simply-supported, while in-plane ones are based on the assumption of unloaded edges free to translate but forced to remain straight. Loading conditions of uniaxial compression are considered, and the load is introduced via prescribed displacement Δu. A sketch of the structure is reported in Figure 1.

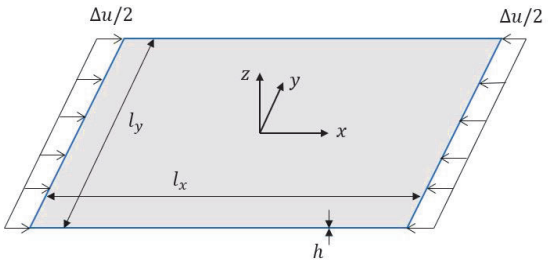

Figure 1. Sketch of the plate.

The problem is formulated by considering von Kármán-type geometric nonlinearity. This assumption leads to a non-objective strain measure, so care is needed when using this approximation. Previous studies have proven its validity when boundary conditions allow significant postbuckling stress redistribution [12], as in the case investigated here.

The mixed formulation relies upon the unitary functional presented in [9,10,11], where the unknowns are the out-of-plane displacement and the Airy stress function. Specifically, the functional reads:

$$\Pi^* = \Pi_m + \Pi_b + \Pi_{nl} + \Pi_{imp} + \Pi_{load} \tag{1}$$

with:

$$\Pi_m = -\frac{1}{2}\int_{\bar{S}} [r^4 a_{11}(\xi,\eta)F_{,\eta\eta}^2 + 2r^2 a_{12}(\xi,\eta)F_{,\xi\xi}F_{,\eta\eta} + a_{22}(\xi,\eta)F_{,\xi\xi}^2 + r^2 a_{66}(\xi,\eta)F_{,\xi\eta}^2 - 2r^3 a_{16}(\xi,\eta)F_{,\eta\eta}F_{,\xi\eta} - 2r a_{26}(\xi,\eta)F_{,\xi\xi}F_{,\xi\eta}]d\bar{S} \tag{2}$$

$$\Pi_b = \frac{1}{2}\int_{\bar{S}}[D_{11}(\xi,\eta)w_{,\xi\xi}^2 + 2r^2D_{12}(\xi,\eta)w_{,\xi\xi}w_{,\eta\eta} + r^4D_{22}(\xi,\eta)w_{,\eta\eta}^2 + 4r^2D_{66}(\xi,\eta)w_{,\xi\eta}^2 + 4rD_{16}(\xi,\eta)w_{,\xi\xi}w_{,\xi\eta} + 4r^3D_{26}(\xi,\eta)w_{,\eta\eta}w_{,\xi\eta}]d\bar{S} \quad (3)$$

$$\Pi_{nl} = \frac{1}{2}r^2\int_{\bar{S}}\left[F_{,\eta\eta}w_{,\xi}^2 + F_{,\xi\xi}w_{,\eta}^2 - 2F_{,\xi\eta}w_{,\xi}w_{,\eta}\right]d\bar{S} \quad (4)$$

$$\Pi_{imp} = -r^2\int_{\bar{S}}\left[F_{,\eta\eta}w_0w_{\xi\xi} - 2F_{,\xi\eta}w_0w_{\xi\eta} + F_{,\xi\xi}w_0w_{\eta\eta}\right] \quad (5)$$

$$\Pi_{load} = -\frac{l_x r^2}{4}\left(\int_{-1}^{1}F_{,\eta\eta}\ \ |_{\xi=-1}d\eta + \int_{-1}^{1}F_{,\eta\eta}\ \ |_{\xi=1}d\eta\right)\Delta u \quad (6)$$

where $r=l_x/l_y$ is the plate aspect ratio, w_0 represents the initial imperfection, while D_{ik}, a_{ik} are the bending stiffness and the membrane compliance according to the standard notation used for laminate analysis. Integration is carried out in the nondimensional domain $(\xi,\eta) \in [-1\ 1] \times [-1\ 1]$.

The variational principle based on Eq. (1) requires the first variation of Π^* to be zero. This leads to the governing equations for the problem, which are the out-of-plane equilibrium and the in-plane compatibility.

Solution by Accounting for Anisotropy Effects

Previous studies suggested the use of the Ritz method as an effective mean for obtaining an approximate solution with improved computational efficiency. In particular, Wu et al. [10] proposed an approach based on Legendre polynomials. Despite its effectiveness, this approach cannot account for membrane anisotropy. Strategies for overcoming this restriction have been discussed in [11] based on Lagrange multipliers. Here, we propose a relatively straightforward approach that can be used to account for the above mentioned elastic couplings with no need to resort to Lagrange multipliers.

The out-of-plane deflection is approximated as presented in [10,11]. A new strategy is proposed for the description of the Airy stress function. In particular, the following requirements need to be fulfilled:

1. the edge force N_{x0} must be allowed to have different distributions at $\xi = \pm 1$. Similarly, N_{y0} must be allowed to have different distributions at $\eta = \pm 1$.
2. shearing force at all the edges, N_{xy0}, must be equal to zero.
3. the lateral edges are free to move but constrained to remain straight, thus: $\int_{-1}^{1} N_{y0}d\xi = 0$

An expansion respectful of these three conditions is carried out as:

$$F(\xi,\eta) = F_0(\xi,\eta) + F_1(\xi,\eta) + F_2(\xi,\eta) \quad (7)$$

where:

$$F_{0,\xi}(\xi,\eta) = -\frac{1}{2}X_1(\eta)(1-\xi^2)\sum_{j=0}^{J}d_{1j}M_j(\xi) - \frac{1}{2}X_2(\eta)(1-\xi^2)\sum_{j=0}^{J}d_{2j}M_j(\xi) \quad (8)$$

$$F_{1,\eta}(\xi,\eta) = \frac{l_y^2}{4}\bar{N}_x\eta - \frac{1}{2}X_1(\xi)(1-\eta^2)\sum_{k=0}^{K}c_{1k}L_k(\eta) - \frac{1}{2}X_2(\xi)(1-\eta^2)\sum_{k=0}^{K}c_{2k}L_k(\eta) \quad (9)$$

and:

$$X_1(\xi) = \begin{cases} 1 - \dfrac{(\xi+1)^2}{2}, & -1 \le \xi < 0 \\ \dfrac{(\xi-1)^2}{2}, & 0 \le \xi \le 1 \end{cases} \quad (10)$$

$$X_2(\xi) = \begin{cases} \dfrac{(\xi+1)^2}{2}, & -1 \le \xi < 0 \\ 1 - \dfrac{(\xi-1)^2}{2}, & 0 \le \xi \le 1 \end{cases} \quad (11)$$

The functions X_1 and X_2 can be either 1 or 0 at $\xi = \pm 1$, and their derivatives at $\xi = \pm 1$ are zero. These properties are exploited to model the skewness in the internal forces and to satisfy boundary conditions, too.

The coefficients $d_{1j}, d_{2j}, c_{1k}, c_{2k}, \overline{N}_x$ are the new unknowns to be calculated by minimizing the unitary functional.

Damage Model

The Ritz formulation presented above allows postbuckling simulations to be carried out. Aiming at gathering insights into the failure mechanisms of postbuckled panels, a damage model is implemented. In this regard, the failure load of the structure can be estimated with an approach that is more physically sound than simpler strategies, such as the first ply failure criterion.

The constitutive law of each orthotropic ply composing the stacking is expressed as:

$$\boldsymbol{Q_d} = \frac{1}{D}\begin{bmatrix} (1-d_f)E_1 & (1-d_f)(1-d_m)v_{21}E_1 & 0 \\ (1-d_f)(1-d_m)v_{12}E_2 & (1-d_m)E_2 & 0 \\ 0 & 0 & D(1-d_s)G_{12} \end{bmatrix} \tag{12}$$

where three damage variables, d_f, d_m, d_s are introduced to represent fiber, matrix, and shear failure modes, and:

$$D = 1 - (1-d_f)(1-d_m)v_{12}v_{21} \tag{13}$$

It is assumed that the damage variable for the shear, d_s, is not independent and is expressed as a function of two other damage variables:

$$d_s = 1 - (1-d_f)(1-d_m) \tag{14}$$

Hashin and Rotem criteria are employed to predict damage initiation. This criterion has been suggested in past studies, e.g. [21,23,24]. Specifically, the Hashin and Rotem criterion distinguishes between failure modes based on the following set of subcriteria:

$$\begin{aligned} &\sigma_{11} \geq 0 && F_{ft} = \left(\frac{\sigma_{11}}{X_t}\right)^2 = 1 \\ &\sigma_{11} < 0 && F_{fc} = \left(\frac{\sigma_{11}}{X_c}\right)^2 = 1 \\ &\sigma_{22} \geq 0 && F_{mt} = \left(\frac{\sigma_{22}}{Y_t}\right)^2 + \left(\frac{\tau_{12}}{S_L}\right)^2 = 1 \\ &\sigma_{22} < 0 && F_{mc} = \left(\frac{\sigma_{22}}{Y_c}\right)^2 + \left(\frac{\tau_{12}}{S_L}\right)^2 = 1 \end{aligned} \tag{15}$$

where X_t, X_c, Y_t, Y_c, S_L are the strength of material in the directions fiber extension, fiber compression, matrix tension, matrix compression and shear, respectively.

As per the approach proposed in [5], the material properties are decreased linearly once damage initiation occurs. The evolution law is expressed in terms of equivalent stress, σ_{eq}, and equivalent strain, ϵ_{eq}. For both the fiber and matrix in tension and compression, they are defined as:

$$\begin{aligned} &\sigma_{11} \geq 0 && \epsilon_{eq.ft} = \langle \epsilon_{11} \rangle && \sigma_{eq.ft} = \frac{\langle \sigma_{11} \rangle \langle \epsilon_{11} \rangle}{\epsilon_{eq.ft}} \\ &\sigma_{11} < 0 && \epsilon_{eq.fc} = \langle -\epsilon_{11} \rangle && \sigma_{eq.fc} = \frac{\langle -\sigma_{11} \rangle \langle -\epsilon_{11} \rangle}{\epsilon_{eq.ft}} = \langle -\sigma_{11} \rangle \\ &\sigma_{22} \geq 0 && \epsilon_{eq.mt} = \sqrt{\langle \epsilon_{22} \rangle^2 + \gamma_{12}^2} && \sigma_{eq.mt} = \frac{\langle \sigma_{22} \rangle \langle \epsilon_{22} \rangle + \tau_{12}\gamma_{12}}{\epsilon_{eq.mt}} \\ &\sigma_{22} < 0 && \epsilon_{eq.mc} = \sqrt{\langle -\epsilon_{22} \rangle^2 + \gamma_{12}^2} && \sigma_{eq.mc} = \frac{\langle -\sigma_{22} \rangle \langle -\epsilon_{22} \rangle + \tau_{12}\gamma_{12}}{\epsilon_{eq.mc}} \end{aligned} \tag{16}$$

The Macaulay bracket operator is denoted by ⟨⟩.The damage variables d_i evolve based on the stress-strain relation shown in Figure 2, where ϵ_{eq}^{0} is the equivalent strain at which the damage criteria for the corresponding mode is satisfied, and ϵ_{eq}^{f} is the one at which the material is completely damaged for that mode. The area below the graph is the fracture energy, G^c.

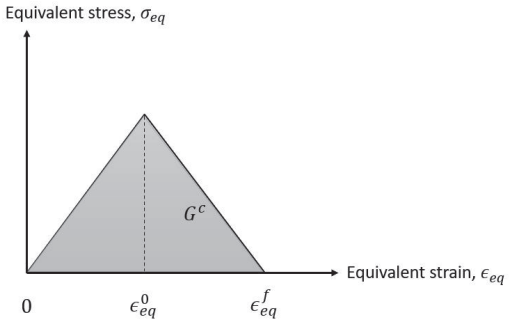

Figure 2. Equivalent strain/stress for linear damage evolution law.

The strain ϵ_{eq}^{f} can be related to ϵ_{eq}^{0} either by specifying the energy dissipation during damage, G^c, or simply with a factor α:

$$\epsilon_{eq}^{f} = \alpha \epsilon_{eq}^{0} \tag{17}$$

In this work, a value of $\alpha = 2$ has been used for each of failure mode [6]. When damage is detected in the fiber or matrix direction, depending on whether the stress state is tensile or compressive, the corresponding damage variable, $d_i$is calculated with the following formulation:

$$d_i = \frac{\epsilon_{eq}^{f}(\epsilon_{eq} - \epsilon_{eq}^{0})}{\epsilon_{eq}(\epsilon_{eq}^{f} - \epsilon_{eq}^{0})} \tag{18}$$

Results

In this section, exemplary results are presented to illustrate the capabilities of the method. In the first part, postbuckling results are presented to show the ability of the proposed method to capture skewness in postbuckling membrane resultants. This effect is crucial to guarantee accurate failure predictions. In the second part, a parametric study is conducted on different VS configurations and failure loads are reported based on the application of PFA.

In all the tests, the material properties are those summarized in Table 1, while the ply strengths are given in Table 2 [1,13].

Table 1. Carbon/epoxy engineering properties.

E_{11} (GPa)	E_{22}(MPa)	G_{12}(MPa)	ν_{12}
150	9080	5290	0.32

Table 2. Ply strenghts.

X_T(MPa)	X_C(MPa)	Y_T(MPa)	Y_C(MPa)	S_L(MPa)
2323	1200	160.2	199.8	130.2

The plates are square with dimension equal to 1000 mm and total thickness fixed to 9.6 mm. Simply-supported boundary conditions are considered. Imperfections are introduced with a shape equal to the first buckling mode and maximum amplitude equal to 0.096 mm, corresponding to 1% of the plate thickness.

Example 1

In this test case, the plate is characterized by the stacking $[\pm\langle 0|45\rangle]_{3S}$, where use is made of the notation proposed in [3]. This configuration is characterized by a non-null degree of bending/twisting coupling, that is quantified by referring to the nondimensional parameters proposed by Nemeth [14]:

$$\gamma = \frac{D_{16}}{\sqrt[4]{D_{11}^3 D_{22}}}, \qquad \delta = \frac{D_{26}}{\sqrt[4]{D_{11} D_{22}^3}} \tag{19}$$

For the laminate at hand, these nondimensional parameters are function of the position due to fiber steering. At the plate center they are null, while they are equal to 0.1895 at the plate loaded edges. These values suggest a significant degree of flexural anisotropy, hence leading to skew buckled shapes. Due to nonlinear coupling between in-plane and out-of-plane response, skew waves promote nonsymmetric membrane resultant redistribution. This effect is illustrated in Figure 3, where the membrane resultant is reported in the deep postbuckling range, at a load level equal to $\Delta u = 10\Delta u_{cr}$. The results are presented by considering two Ritz simulations, both performed with J=K=17: the first, denoted as "Ritz–full", is the one proposed in this work; the second, "Ritz–simplified", is the formulation obtained by neglecting the corrections proposed in Eqs. (8) and (9) and corresponds to the approach proposed in [**Error! Bookmark not defined.**]. The comparison of Figure 3 reports also the results obtained via Abaqus simulations.

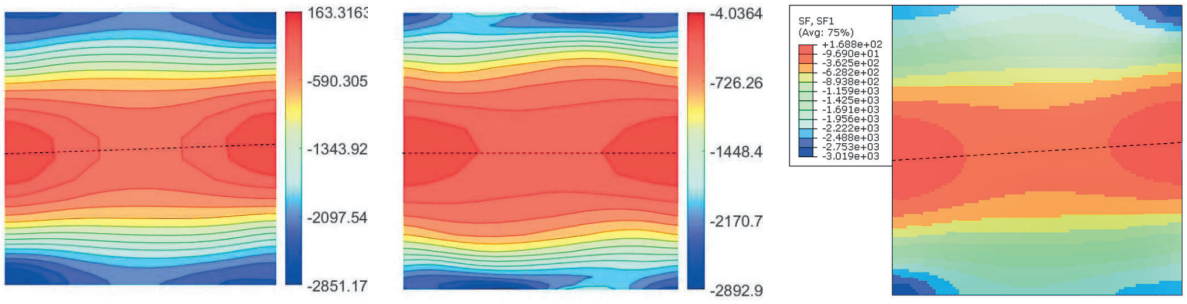

(a) **(b)** **(c)**

Figure 3. Membrane resultant N_{xx} at $\boldsymbol{\Delta u = 10\Delta u_{cr}}$: (a) Ritz– full, (b) Ritz–simplified, (c) Abaqus.

As seen, the pattern is characterized by a certain degree of skewness that is not captured by the Ritz–simplified approach. On the contrary, the proposed formulation allows for an accurate prediction of this effect. The contours illustrate that different membrane resultant patterns are achieved. This, in turn, determines different spots to be the most heavily loaded ones. An appropriate prediction of damage onset is then affected by the ability to account for this elastic coupling effect.

In addition to the mentioned local effects, a proper description of the postbuckling stress redistribution has an effect on the panel global response in the deep postbuckling range. The plot of Figure 4 illustrates the force-shortening curve obtained with different strategies.

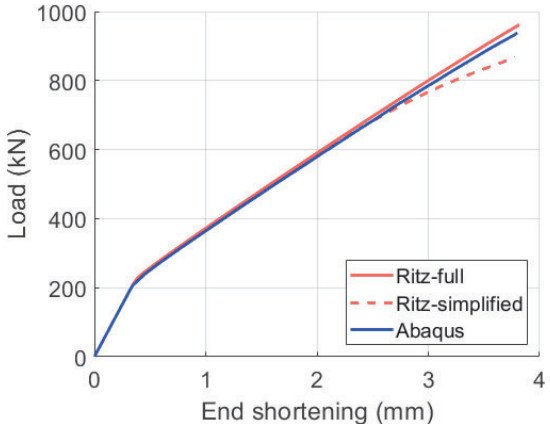

Figure 4. Load-shortening curve.

The curves of Figure 4 illustrate the close agreement between the Ritz– full formulation and the Abaqus results. On the contrary, noticeable discrepancies are observed in the deep postbuckling field when the Ritz-simplified approach is employed.

Example 2

The formulation is applied here to predict the failure loads of different VS configurations using Progressive Failure Analysis. The geometry and the material properties of the plate are the same of the previous example.

The layup is now given by the stacking of 24 plies oriented at $[\pm[\langle 45|T\rangle]_{6S}$, where T is the orientation at the plate edge ranging from 0 to 90 degrees with steps of 10 degrees. Each configuration is associated with different stiffness distributions. In particular, different bending stiffnesses have influence on the buckling load; a combined effect of bending and membrane stiffnessess determines different postbuckling responses. The results are summarized in Figure 5, where Ritz–full computations are compared against costly Abaqus PFA simulations. For the former, results are obtained by using 19 trial functions along both directions.

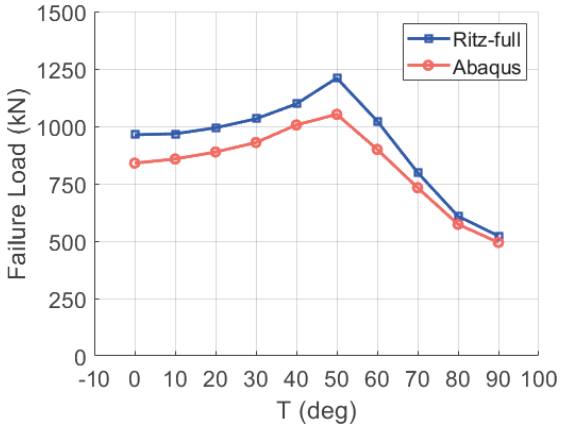

Figure 5. Failure loads for layups $[\pm[\langle \mathbf{45}|\boldsymbol{T}\rangle]_{\mathbf{6}\boldsymbol{S}}$.

The results demonstrate a good matching between Ritz and FEM simulations. Maximum discrepancies of approximately 10% can be noted, which is believed satisfactory owing to the complex combined effects of material and geometric nonlinearities. More important, the Ritz approach is able to predict the trend correctly. This feature is of interest from a design perspective. The proposed tool can be used for preliminary studies aimed at understanding how the response of the plate is affected by changing one or more design parameters. For the problem at hand, the

maximum failure load is achieved for T=50°. Clearly, this configuration does not represent an absolute optimum. Many other requirements – e.g. linear stiffness, postbuckling stiffness, buckling load – would be part of a more realistic design scenario.

For the laminate corresponding to T=0°, the plot of the membrane resultant is reported in Figure 6 at the load level corresponding to the laminate failure.

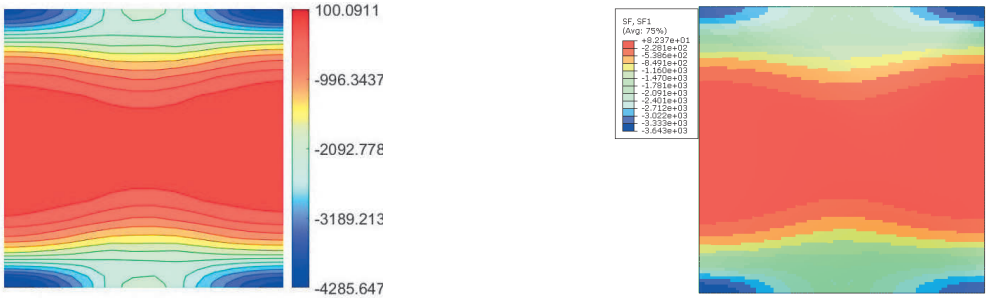

(a) **(b)**

Figure 6. Membrane resultant N_{xx} at failure: (a) Ritz– full, (b) Abaqus.

In this case, the laminate undergoes a damage mechanism that is driven by matrix failure in tension. Specifically, large tensile forces develop at the middle of the transverse edges as a response to the straightness condition. The plot of the corresponding damage variables, d_m, is reported in Figure 7 for the first ply of the stack.

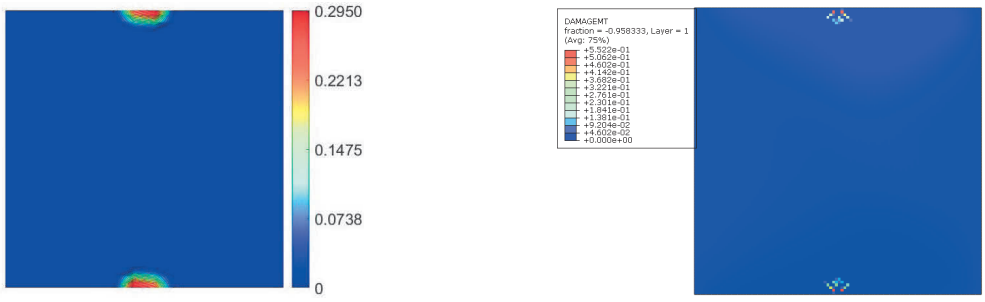

(a) **(b)**

Figure 7. Damage variable d_m: (a) Ritz– full, (b) Abaqus.

The contours of Figure 7 demonstrate the ability of the method to identify the critical spots involved in the failure mechanism. Indeed, both Ritz and Abaqus predictions display similar damaged patterns. In this regards, the proposed Ritz method is a useful mean not only to predict the failure load, but also to gather insight into the whole failure process.

Conclusions

This work presented a novel approach to perform fast preliminary evaluations to estimate the failure load of laminated plates. Advanced configurations with fibers running along curvilinear paths can be considered within the proposed framework. The approach is developed on the basis of a mixed variational approach, and the Ritz method is combined with a linear degradation model.

This approach can accurately predict the laminate response, not only in the initial postbuckling field, but up to the deep postbuckling range, where material failure usually takes place. To achieve this capability, a refined approximation of the stress function has been proposed to accurately capture stress redistribution effects induced by bending/twisting coupling. This capability is of crucial importance to guarantee an accurate prediction of the failure load, as well as identifying the regions involved in the failure process. The comparisons against Abaqus simulations

demonstrate the excellent quality of the predicted internal stresses and failure loads. The potential of the approach to investigate the effects of fiber steering on the laminate failure load has been shown with a parametric study. More realistic design scenarios including multiple design requirements will be investigated as part of future investigations.

References

[1] C. Bisagni, R. Vescovini and C.G. Dávila, Single-stringer compression specimen for the assessment of damage tolerance of postbuckled structures, Journal of Aircraft 48 (2011) 495-502. https://doi.org/10.2514/1.C031106

[2] M.W. Hyer and R.F. Charette, Use of curvilinear fiber format in composite structure design, AIAA Journal 29 (1991) 1011-1015. https://doi.org/10.2514/3.10697

[3] Z. Gürdal, B.F. Tatting and C.K. Wu, Variable stiffness composite panels: effects of stiffness variation on the in-plane and buckling response. Composites Part A: Applied Science and Manufacturing 39 (2008) 911-922. https://doi.org/10.1016/j.compositesa.2007.11.015

[4] A. Matzenmiller, J. Lubliner and R.L. Taylor, A constitutive model for anisotropic damage in fiber-composites, Mechanics of Materials 20 (1995) 125-152. https://doi.org/10.1016/0167-6636(94)00053-0

[5] I. Lapczyk and J.A. Hurtado, Progressive damage modeling in fiber-reinforced materials, Composites Part A: Applied Science and Manufacturing 38 (2007) 2333-2341. https://doi.org/10.1016/j.compositesa.2007.01.017

[6] Q.J. Yang and B. Hayman, Simplified ultimate strength analysis of compressed composite plates with linear material degradation, Composites Part B: Engineering 69 (2015) 13-21. https://doi.org/10.1016/j.compositesb.2014.09.016

[7] S.A.M. Ghannadpour and M. Shakeri, Application of a new energy-based collocation method for nonlinear progressive damage analysis of imperfect composite plates, Thin-Walled Structures 147 (2020) 106369. https://doi.org/10.1016/j.tws.2019.106369

[8] D. Campagna, A. Milazzo, I. Benedetti and V. Oliveri, A non-linear Ritz method for progressive failure analysis of variable angle tow composite laminates, Mechanics of Advanced Materials and Structures (2022) 1-14. https://doi.org/10.1080/15376494.2022.2134951

[9] C. Bisagni and R. Vescovini, Analytical formulation for local buckling and post-buckling analysis of stiffened laminated panels, Thin-Walled Structures 47 (2009) 318-334. https://doi.org/10.1016/j.tws.2008.07.006

[10] Z. Wu, G. Raju and P.M. Weaver, Postbuckling analysis of variable angle tow composite plates, International Journal of Solids and Structures 50 (2013) 1770-1783. https://doi.org/10.1016/j.ijsolstr.2013.02.001

[11] Z. Wu, G. Raju and P.M. Weaver, Buckling of VAT plates using energy methods, 53rd AIAA/ASME/ASCE/AHS/ASC Structures, Structural Dynamics and Materials Conference 20th AIAA/ASME/AHS Adaptive Structures Conference 14th AIAA, 2012. https://doi.org/10.2514/6.2012-1463

[12] G. Garcea, A. Madeo and R. Casciaro. Nonlinear fem analysis for beams and plate assemblages based on the implicit corotational method, Journal of Mechanics of Materials and Structures 7 (2012) 539-574. https://doi.org/10.2140/jomms.2012.7.539

[13] P.P. Camanho, P Maimí and C.G. Dávila, Prediction of size effects in notched laminates using continuum damage mechanics, Composites Science and Technology 67 (2007) 2715-2727. https://doi.org/10.1016/j.compscitech.2007.02.005

[14] M.P. Nemeth, Importance of anisotropy on buckling of compression-loaded symmetriccomposite plates, AIAA Journal 24 (2012), 1831-1835. https://doi.org/10.2514/3.9531